High Resolution Starry Night Panoramas

Grant Yang
EE368: Digital Image Processing
Electrical Engineering, Stanford University
Stanford, California
granty@stanford.edu

***Abstract*—A method was presented for combining multiple exposures of the night sky to create a single panorama of the scene. The algorithm is capable of compensating for celestial motion without significant artifacts in the boundaries between the land and the sky. The images are first segmented into land and sky. Next the locations of probable stars in the image are calculated and used to estimate celestial motion as a local affine transform. The motion of the stars is then compensated by smoothly warping the images using the local transformations. This motion compensation has been integrated into an automatic panorama stitching algorithm which uses spherical projections. The method was demonstrated on a sample dataset.**

Keywords—panorama stitching; image processing; photography

I. INTRODUCTION

Combining astrophotography with panoramic landscapes presents many challenges dealing with image noise and subject motion. Low light levels require the use of long shutter speeds and/or high ISOs in order to acquire sufficient signal. However, high ISOs result in a low signal to noise ratio (SNR), and long exposures are sensitive to thermal noise and hot pixels. Compounding the noise issue, stars are also susceptible to motion blur due to the rotation of the earth. This spatially variant motion precludes the use of longer exposures to improve signal levels. The spatially variant motion blur also complicates panorama stitching.

Current methods for dealing with the rotation of the earth include using a motorized mount, which tracks the apparent motion of the stars, or to increase the field of view using ultra-wide angle lenses. A motorized mount allows the use of much longer exposure without blurring the stars. However, these mounts are expensive and unsuitable for panorama stitching as the movement introduces blur to the foreground elements. Ultra-wide angle lenses decrease the effect of motion at the cost of image resolution. In addition ultra-wide lenses introduce additional lens distortions, which must be modeled for successful panorama stitching.

Combining several short exposures is an alternate solution to the problem of motion and noise. This method increases SNR and avoid blurring and stitching artifacts in the panorama image by introducing a spatially variant registration step[1] into a spherical projection panorama stitching algorithm. By careful definition of the transitions between registration regions, distortion of the foreground elements as well as visible artifacts can be minimized.

II. ALGORITHM

The algorithm combines a series of frames into a panorama image. Each frame may consist of many separate exposures. The longest possible shutter speed without noticeable star trailing should be chosen for each exposure, and the combined exposures for each frame should be sufficient to produce a well-exposed final image. In addition the frames are assumed to have approximately 30 percent overlap, and to be taken by rotation about the no-parallax point to allow for error-free panorama stitching.

A. Segmentation of Astronomical and Terrestrial Elements

The astronomical and terrestrial elements of each frame were segmented based on brightness differences. The algorithm averages all the exposures in each frame without registration. This increases the SNR of the image allowing for more accurate segmentation. The blue channel of the averaged frame is thresholded using Otsu's method. The resulting binarized image is inverted, and the largest contiguous region is set to one, while the remaining mask is set to zeros. This eliminates holes in the astronomical portion of the image mask. The resulting mask is then inverted. The largest contiguous region is again set to one while the rest of the mask is set to zero. The result is a binarized mask where ones represent the astronomical elements and zeros represent terrestrial elements of the scene without holes in either region.

B. Finding Star Keypoints

Potential stars were found in the sky using a thresholding operation on each exposure. The algorithm assumes that stars represent the brightest regions in the sky. The threshold was chosen such that approximately five hundred regions were found in each exposure. The centroid and area of each region were calculated. The potential star locations were defined as the centroid of the regions with areas less than 1000 pixels. Since the stars are the same scale and approximate orientation in each exposure, the scale and orientation of the keypoints were set to 15 pixels and 0 degrees respectively.

C. Combining Exposures

SIFT descriptors were calculated for each of the keypoints found in Step B. The image was split into six segments, and the affine transformation between exposures was calculated for each segment using SIFT keypoint matching and RANSAC. If insufficient RANSAC matches were found, the previous successfully calculated transform was propagated to

the next segment. In order to avoid discontinuities between segments, cubic interpolation was performed to provide a smooth transition between image segments. The registered exposures were then averaged in order to increase the SNR of each frame.

D. Spherical Projection

The denoised images were warped onto a spherical surface[2].

$$x' = f \cdot \tan\left(\frac{x}{s}\right) \quad (1)$$

$$y' = f \cdot \tan\left(\frac{y}{s}\right) \sec\left(\frac{x}{s}\right) \quad (2)$$

(x', y') denotes the new coordinates of the pixel located at (x, y), f is the focal length of the imaging system in pixels, and *s,* is a scale factor. In order to preserve scaling of the projected image, *s* was chosen to equal *f.* A spherical projection allows alignment of the frames using a purely translational model at the expense of the preservation of straight lines. Because starry night images are primarily taken outdoors in remote locations, distortion of straight lines will generally be unoticeable in the final image.

E. Register Frames

The relationship between the spherically projected frames were calculated by using SIFT and RANSAC. The resulting transformations were used to transform the spherically projected images to their final locations in the panorama.

F. Register Stars

Although the homographies calculated in Step E provide good alignment of the landscape portions of the image, the stars are poorly registered due to motion between frames. This is corrected by repeating Steps A-C on the transformed images.

G. Blending Images

The fully registered images from Step F were blended together to form the final panorama. In order to avoid noticeable discontinuities between frames, a weighting function was applied to each frame according to equation 3 [3],

$$I_c = \frac{\sum_{i=1}^{N} F_i W_i}{\sum_{i=1}^{N} W_i} \quad (3)$$

where N denotes the number of frames, I_c denotes the combined image, F_i denotes the i^{th} frame and W_i denotes the weighting function. A good weighting function was found to be the inverse cube of the Euclidean distance from the center of the frame as seen in equation (4), where (x_{ci}, y_{ci}) denotes the center of the i^{th} frame.

$$(W_i)_{xy} = ((x - x_{ci})^2 + (y - y_{ci})^2)^{-3/2} \quad (4)$$

H. Sharpening and Contrast

The final step in the algorithm was to perform a Weiner deconvolution to remove image blurring due to slight inaccuracies in the registration steps and lens imperfections. The blur was modeled as a Gaussian point spread function with a standard deviation of 1.6 pixels. The power spectral density of the noise was measured using an ROI of a featureless portion of the sky. The contrast and exposure of the final image was also slightly altered to optimize visual appeal.

A summary of the panorama generation algorithm has been included below.

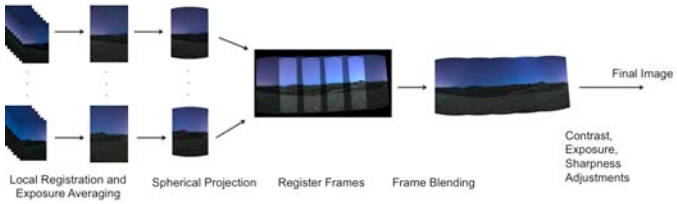

Fig. 1. Summary of the panorama generation algorithm

III. Results and Discussion

A. Image Acquisition

Images were acquired using a Sony A77 DSLT with a 16-50mm f2.8 SSM lens set to 16mm. The camera was mounted vertically on a tripod such that the entrance pupil of the lens coincided with the axis of rotation in order to eliminate parallax errors. The setup is shown below.

Fig. 2. Panorama imaging system

In order to maximize signal while avoiding motion blur, the shutter speed was set to 15 seconds. Five frames were taken with a 30° rotation between each frame. Six separate 15 second exposures at ISO 3200 were taken for each frame. The images encompassed a total field of view of 172°. The specifications of the image acquisition have been summarized in Table 1 below.

TABLE I. Image Acquisition System

Camera	Sony A77	**Lens**	Sony 16-50mm f2.8

Sensor Size	23.5x15.6 mm	**Focal Length**	16mm
Image Dimensions	6000x4000	**# of Frames**	5
ISO	3200	**Exposures/Frame**	6
Shutter Speed	15 sec	**Effective FOV**	172º

B. Image Processing

The images were processed in MATLAB r2013b with the vl_feat library to generate a panorama with a 172º field of view. The image segmentation algorithm in Step A was applied to each frame. The algorithm was found to be effective for the example dataset, yielding consistent results across all five frames. This indicates a degree of robustness to variations in lighting conditions as the amount of light pollution varied between frames. An example of the output along with several intermediate steps of the segmentation algorithm is shown below.

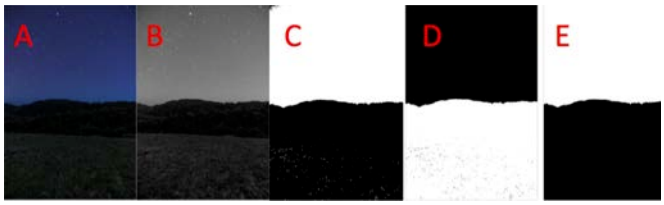

Fig. 3. (A) Averaged frame (B) Blue channel of the averaged frame (C) Binarized mask using Otsu's method (D) Hole filling in the astronomical portion of the image mask (E) Final mask after hole filling in the terrestrial portion of the mask

Next star keypoints were generated according to the algorithm in Step B The resulting keypoints have been displayed in Fig. 4 below.

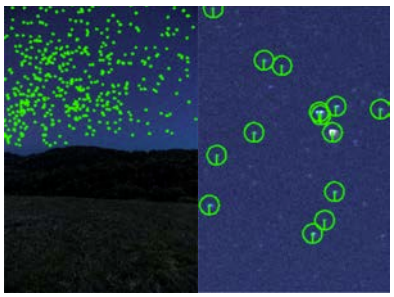

Fig. 4. SIFT keypoints generated according to the algorithm in Step B (left) and a close up of the keypoints detected in a small region of sky (right).

The stars were registered by matching the SIFT descriptors to combine the six exposures into an image with improved signal to noise ratio. As seen in Fig. 5, the noise variance was found to be inversely proportional to the number of exposure averages.

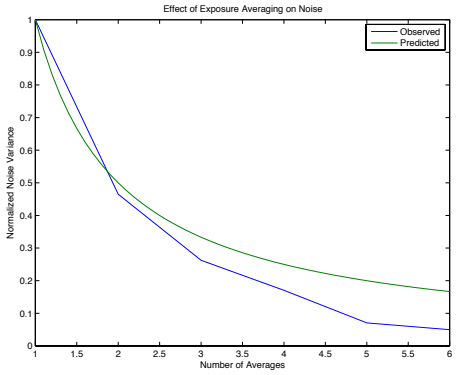

Fig. 5. Normalized noise variance as a function of the number of exposures. The noise variance is expected to decay as *1/N* for zero mean Gaussian noise

As seen in Fig. 6, the measurable drop in noise was visually apparent in the image. By averaging the frames, the luminance noise, which appears as a mottled sky in the original image is considerably reduced. There was also a visible improvement in the clarity of dimmer stars.

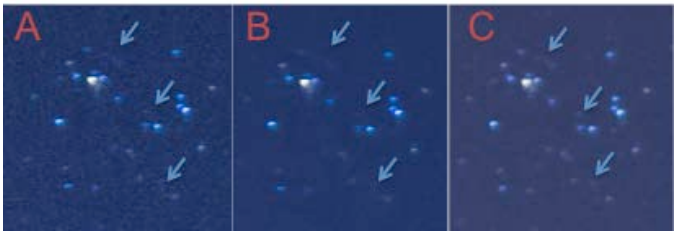

Fig. 6. Arrows indicate stars which have been recovered using exposure averaging (C) compared to original exposure (A), and noise reduction in Lightroom 5.1 (B)

Also shown in Fig. 6 is a comparison between the image averaging used in this algorithm and the noise reduction algorithms included with the popular image processing software Lightroom 5.1. As seen in Fig. 6, the Lightroom noise reduction reduces visual noise at the cost of smoothing out many of the dimmer stars.

The registration algorithm in Step C was also successful at avoiding motion blur as seen in Fig. 7a. This allows the generation of much cleaner images without the star trailing which would result from a single long exposure as seen in Fig. 7b.

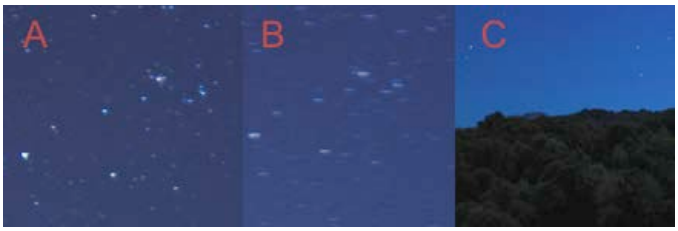

Fig. 7. Motion correction (A) results in a substantial improvement in sharpness over the uncorrected image (B). The spatially variant technique results in minimal noticeable artifacts at image boundaries (C)

The interpolation scheme used to blend the spatially variant registrations performed well on the data set. There were minimal artifacts between transition regions as seen in Fig. 7c, and the algorithm was able to successfully accommodate movements of up to 15-20 pixels without significant artifacts. Ghosting of image elements due to the interpolation was found to occur when more extreme motion was detected.

The combined exposures were stitched into a panorama using a spherical projection. The effect of the blending algorithm on the panorama was explored by altering the weighting used in equation 3. As seen in Fig. 8, faster decaying weighting functions resulted in smoother transition regions in the final panorama.

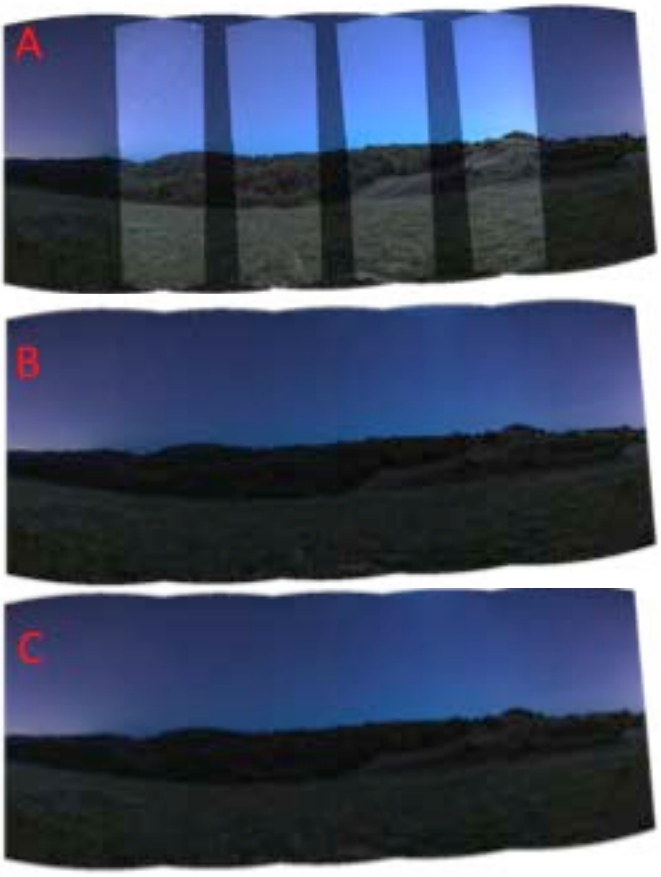

Fig. 8. Panorama without blending (A), inverse Euclidean distance (B), inverse distance squared (C), and inverse distance cubed (D) showing smoother transitions for faster decaying weighting functions

The stitched panorama image was deblurred using Weiner deconvolution in order to counteract blur induced by slight registration mismatches and optical imperfections in the imaging system. As seen in Fig. 9, the Weiner deconvolution increased the sharpness of the final image.

Fig. 9. The sharpness of the final image (right) was improved compared to the original image (left) by applying a Weiner deconvolution

IV. Future Work

More work is needed in order to make the algorithm faster and more robust. More image sets should be tested in order to demonstrate that the algorithm is useable under a variety of conditions. Furthermore, the algorithm could be made more autonomous by selecting appropriate thresholds for the segmentation and star finding steps automatically. The algorithm should also be made adaptable to a variety of imaging systems by automatically compensating for changes in sensor size and focal length.

The algorithm should also be ported to a programming language more suitable for high resolution images. MATLAB was very useful as a development language for algorithms, but tended to crash when working on high resolution datasets.

Finally, the algorithm should be demonstrated on more impressive input images. The images used in this report were taken with significant light pollution from both city lights and the moon overpowering many of the stars and the Milky Way. The algorithm should be capable of more impressive images given the proper inputs.

V. Conclusion

The panorama stitching program implemented in this paper successfully overcomes two major obstacles to generating night sky panoramas: low SNR and motion blur. By including spatially variant registration steps into the panorama workflow, the algorithm was able to combine several shorter exposures into a lower noise final image without motion artifacts. The algorithm was applied to a sample image set and demonstrated significant improvements in image quality.

Acknowledgment

The author would like to acknowledge the EE368 course staff for their assistance with the project. He would also like to thank Marian Yang for accompanying him on his photography expeditions at odd hours of the night.

References

[1] M. Brown and D. Lowe, "Automatic Panoramic Image Stitching Using Invariant Features," International Journal of Computer Vision, Aug. 2007.

[2] Szeliski, Richard, "Image Alignment and Stitching, A Tutorial," Microsoft Research., Redmond, WA, Tech. Rep., MSR-TR-2004-92, 2006.

[3] Heung-Yeung Shum and Richard Szeliski. Construction of panoramic mosaics with global and local alignment. *International Journal of Computer Vision*, 36(2):101-130, February 2000. Erratum published July 2002, 48(2):151-152.